Surface Characteristics on the Stress Corrosion Cracking of Alloy 690TT in Lead-containing Caustic Solution

Byung-Hak Moon*, Dong-Jin Kim, Hong-Pyo Kim, Seong-Sik Hwang
Nuclear Materials Research Division, Korea Atomic Energy Research Institute (KAERI),
Yuseong-Gu, Daejeon, 305-353
**Corresponding author: mbh@kaeri.re.kr*

1. Introduction

Nickel-based Alloy 690 is a technologically important material widely used a structural material for steam generator tubes in pressurized water reactors (PWRs). Higher chromium content than Alloy 600 endows an improved corrosion resistance [1,2], and failures of Alloy 690 tubes have rarely been reported. However, Alloy 690 has also been reported to be susceptible to stress corrosion cracking (SCC), intergranular attack, hydrogen embrittlement and lead-induced SCC in caustic environments.

Its long-term corrosion behavior under service conditions is still a highly concerned issue. For example, corrosion leads to nickel release in water, which can be activated into ^{58}Co in the nuclear core under a neutronic flux, and as such increases the global radioactivity of the primary circuit of PWR [3]. Corrosion is also the primary cause for the initiation and growth of stress corrosion cracking [4]. The characteristics of the oxide films formed on an alloy, including chemical composition, microstructure and thickness, etc., determine the protect ability of the oxide film and thus plays a crucial role in the corrosion behavior [5-8]. A couple of material and environment relevant factors influence the oxide film characteristics. In addition to the chemical composition and microstructure of the alloy, water chemistry and surface finishing condition are two key factors that can vary the characteristics of the oxide film.

In this study, we investigated the surface characteristics on the stress corrosion cracking of alloy 690TT in lead-containing caustic solution.

2. Experimental

The chemical compositions of Alloy 690TT used in the present work are given in Table 1.

The slow strain rate tensile (SSRT) test is known to take a relatively shorter time and show better reproducibility compared to other test methods. The SSRT tests were carried out using a Ni autoclave of 0.5 gallons at 315°C and an open circuit potential. Tensile specimens having a gauge length of 25.4mm were used for SSRT. The specimens were cleaned using acetone immediately before loading. The test environments for SSRT were performed in a lead-containing NaOH solution at 315°C. The environment cell was designed such that the gauge length remained immersed in the test environment during the entire test duration.

In the present study, all specimens were tested with the strain rate of $2 \times 10^{-7} s^{-1}$. The cell was filled with the test solution before starting the machine. The load was applied by employing the constant extension rate mode. A pre-load of ~50lbs was applied to take care of the machine slack. The load and extension were monitored continuously by a load cell and LVDT. As there was no extension meter attached to the specimen gauge length, SSRT tests produced apparent stress-strain curves.

The fracture surfaces were washed in distilled water and rinsed with acetone, before examination using a scanning electron microscope (SEM). From the SEM observations, the crack morphology and SCC areas were determined. Detailed cross-section characteristics were analyzed using transmission electron microscopy (TEM). Thin-foil samples for TEM observations were prepared using a Helios 600 focused ion beam (FIB) with Ga ion sputtering after a thin layer of protective Pt was coated on the oxide surface. Scanning transmission electron microscopy (STEM) observations were performed with a Tecnai G2 F20 TEM instrument equipped with an energy-dispersive spectroscopy (EDS) system operating at 200 kV.

3. Results and discussion

Fig. 1 a-b show the surface morphology of the alloy 690TT specimens after the SSRT experiments. As shown in Fig. 1b, following the exposure in a lead-containing NaOH solution, the specimen was covered by irregularly shaped lead particles, which appear to be randomly packed on the surface. The size of the lead particles is inhomogeneous. SCC of 4% on the fractured surface occurred in a 1M NaOH solution, while 16% of the surface area fractured in lead-containing 1M NaOH solution.

Fig. 2 shows the stress-strain curves of the alloy 690TT tested in 1M NaOH and lead-containing 1M NaOH solution. The El and ultimate tensile strength (UTS) of alloy 690TT tested in a 1M NaOH solution were approximately 52.5% and 611MPa, respectively, whereas in a lead-containing 1M NaOH solution, they were approximately 34.2% and 537MPa, respectively. There is an apparent difference in the El and UTS of the 1M NaoH solution and lead-containing 1M NaOH solution.

EDS line-scan analyses across the inner oxide layer were also conducted to show the composition profiles. With regard to the oxide layer formed in a 1M NaOH solution, Fig. 3 shows that Ni is enriched at outermost oxide layer, followed by Cr enriched oxide layer up to 1μm thickness while the alternative layers of Ni and Cr enriched layer whose oxygen content is lower than that of former layer are observed up to 2μm thickness. Fig. 4 shows the composition profile of the oxide layer formed in a lead-containing 1M NaOH solution. Ni is depleted at outermost oxide and Cr enriched oxide is not found easily in the oxide due to Pb unlike the results obtained in 1M NaOH without Pb. However, thick layer whose oxygen content is around 10wt% is also observed, similar to that of the oxide formed in a 1M NaOH solution.

4. Conclusions

From the SSRT tests and SEM images, the SCC increased from 4 to 16% for alloy 690TT when a lead content of 10000ppm was added to a 1M NaOH solution. The oxides formed in 1M NaOH solution were observed as a function of PbO addition.

REFERENCES

[1]K.H. Lee, G. Cragnolino, D.D. MacDonald, Effect of heat treatment applied potential on the caustic stress corrosion cracking of Inconel 600, Corrosion, Vol. 41, p.540, 1985.
[2] W.K. Lai, Z.S. Smialowska, Effect of heat treatment on the behavior of Alloy 600 in lithiated water containing dissolved hydrogen at 25-350°C, Corrosion, Vol. 47, p.40, 1991.
[3] M. Sennour, L. Marchetti, F. Martin, S. Perrin, R. Molins, M. Pijolat, A detailed TEM and SEM study of Ni-base alloys oxide scales formed in primary conditions of pressurized water reactor, J. Nucl. Mater, Vol. 402, p.147, 2010.
[4]Z.S. Smialowska, W.K. Lai, Z. Xia, Oxide films formed on Alloy 600 in lithiated water at 25− 350°C, Corrosion Vol. 46, p. 853, 1990
[5] T. Terachi, N. Totsuka, T. Yamada, T. Nakagawa, H. Deguchi, M. Horiuchi, M. Oshitani, Influence of dissolved hydrogen on structure of oxide film on Alloy 600 formed in primary water of pressurized water reactors, J. Nucl. Sci. Technol, Vol. 40, p. 509, 2003.
[6] F. Carette, M.C. Lafont, G. Chatainier, L. Guinard, B. Pieraggi, Analysis and TEM examination of corrosion scales grown on Alloy 690 exposed to pressurized water at 325°C, Surf. Interface Anal, Vol. 34, p.135, 2002
[7] L. Marchetti, S. Perrin, Y. Wouters, F. Martin, M. Pijolat, Photoelectrochemical study of nickel base alloys oxide films formed at high temperature and high pressure water, Electrochim. Acta, Vol. 55, p.5384, 2010.
[8] J. Panter, B. Viguier, J.M. Cloue, M. Foucault, P. Combrade, E. Andrieu, Influence of oxide films on primary water stress corrosion cracking initiation of Alloy 600, J. Nucl. Mater, Vol. 348, p. 213, 2006.

Table 1 Chemical compositions of Alloy 690 TT (wt %)

Material	C	Si	Mn	P	Cr	Ni	Fe	
Alloy690	0.02	0.22	0.32	0.009	29.57	58.9	10.54	
Material	Co	Ti	Cu	Al	B	S	N	Nb
Alloy690	0.01	0.26	0.01	0.019	0.004	0.001	0.017	0.01

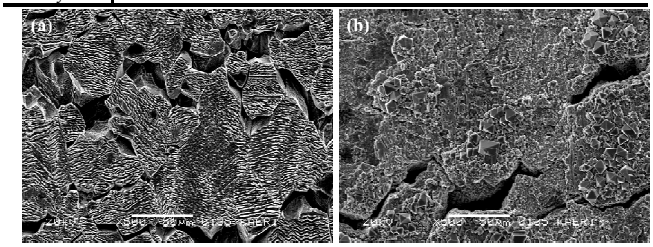

Fig. 1. SEM observation of alloy 690TT after SSRT in 1M NaOH and lead-containing 1M NaOH solution.

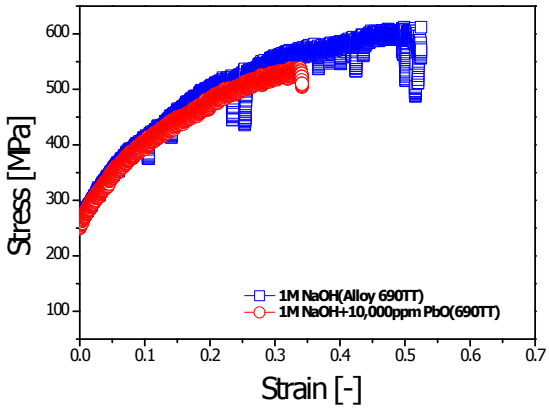

Fig. 2. Stress-strain curves of alloy 690TT after SSRT in 1M NaOH and lead-containing 1M NaOH solution.

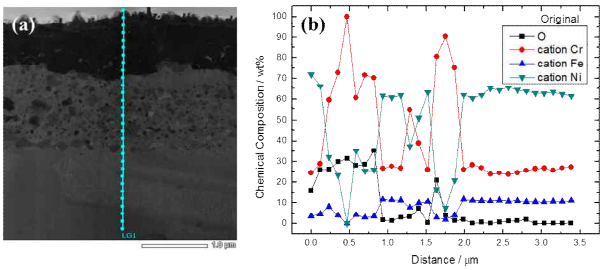

Fig. 3. Elemental concentration profiles across the inner oxide scale of alloy 690TT in 1M NaOH solution. (a) STEM image and (b) EDS measuring points

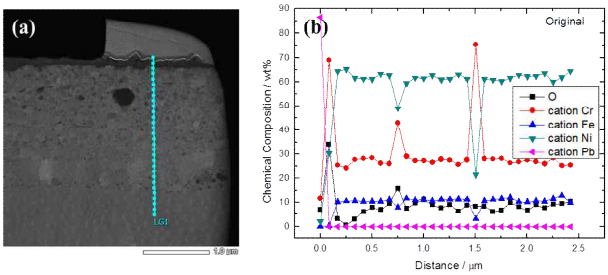

Fig. 4. Elemental concentration profiles across the inner oxide scale of alloy 690TT in lead-containing 1M NaOH solution. (a) STEM image and (b) EDS measuring points